

One step backwards is two steps forward: enhancing the hydrolysis rate of UiO-66 by decreasing [OH-]

Michael J. Katz, Rachel C Klet, Su-Young Moon, Joseph E Mondloch, Joseph T. Hupp, and Omar K. Farha

ACS Catal., Just Accepted Manuscript • DOI: 10.1021/acscatal.5b00785 • Publication Date (Web): 26 Jun 2015

Downloaded from <http://pubs.acs.org> on July 6, 2015

Just Accepted

“Just Accepted” manuscripts have been peer-reviewed and accepted for publication. They are posted online prior to technical editing, formatting for publication and author proofing. The American Chemical Society provides “Just Accepted” as a free service to the research community to expedite the dissemination of scientific material as soon as possible after acceptance. “Just Accepted” manuscripts appear in full in PDF format accompanied by an HTML abstract. “Just Accepted” manuscripts have been fully peer reviewed, but should not be considered the official version of record. They are accessible to all readers and citable by the Digital Object Identifier (DOI®). “Just Accepted” is an optional service offered to authors. Therefore, the “Just Accepted” Web site may not include all articles that will be published in the journal. After a manuscript is technically edited and formatted, it will be removed from the “Just Accepted” Web site and published as an ASAP article. Note that technical editing may introduce minor changes to the manuscript text and/or graphics which could affect content, and all legal disclaimers and ethical guidelines that apply to the journal pertain. ACS cannot be held responsible for errors or consequences arising from the use of information contained in these “Just Accepted” manuscripts.

One step backwards is two steps forward: enhancing the hydrolysis rate of UiO-66 by decreasing [OH⁻]

Michael J. Katz,^a Rachel C. Klet,^a Su-Young Moon,^a Joseph E. Mondloch,^a Joseph T. Hupp,^{*a} Omar. K. Farha^{*a,b}

^aDepartment of Chemistry and the International Institute for Nanotechnology, Northwestern University, 2145 Sheridan Road, Evanston, Illinois 60208–3113, United States.

^bDepartment of Chemistry, Faculty of Science, King Abdulaziz University, Jeddah, Saudi Arabia

ABSTRACT: The rapid destruction of chemical threats such as phosphate-based nerve agents is of considerable current interest. The hydrolysis of the nerve-agent simulant methylparaoxon, as catalysed by UiO-66 and UiO-67, was examined as a function of pH. Surprisingly, even though typical phosphate-ester hydrolysis mechanisms entail nucleophilic attack of the simulant by aqueous hydroxide, the rate of hydrolysis accelerates as the solution pH is lowered. The unexpected behavior is attributed to a pH-dependent composition change followed by ligand substitution at the Zr₆-based node.

KEYWORDS: Metal-Organic Frameworks, Hydrolysis, UiO, Phosphate Nerve Agents, Defects, pH.

Introduction

Metal–Organic Frameworks (MOFs) are a class of porous materials formed via the coordination chemistry between metal-based nodes and polytopic organic linkers.^{1–3} Owing to the tunability of the organic linkers and the wide range of coordination geometry observed across the metals in the periodic table, MOFs are potentially interesting for a wide range of applications such as, but not limited to, gas-storage, chemical separations, sensing, and catalysis.^{4–17}

An area of MOF catalysis of particular interest to us is the hydrolysis of phosphate-based nerve agents (e.g., Sarin, VX, GD, and Soman) and their simulants such as methylparaoxon (Figure 1).^{18–23} The mode of action of these compounds is inhibition of acetylcholinesterase, a hydrolase used to terminate transmission of the neurotransmitter acetylcholine and thereby control muscle response. The mode of action of Sarin begins with phosphorylation of the serine residue at the active site of acetylcholinesterase, upon elimination of the leaving group (nitrophenoxide for methylparaoxon and fluoride for Sarin), that generates robust and biologically inactive phosphoester, which leads to the inhibition of the enzyme and ultimately causes asphyxiation.^{24–33}

In our previous work, we demonstrated that UiO-66,^{34–40} a MOF formed via the coordination of terephthalate dianions to Zr₆O₄(OH)₄¹²⁺ (Figure 1), is capable of hydrolyzing methylparaoxon with a half-life of 35–50 minutes at pH 10.^{18,19} While this half-life is remarkable given the low active catalyst loading (limited to surface-active catalytic sites only), it is too long for applications such as real-time decontamination. To that end, we have investigated the role of bdc (1,4-benzene dicarboxylate) functionalization, linker length, and linker denticity on the overall hydrolysis rate. We have observed that in comparison to UiO-66, UiO-66-NH₂ has a 20-fold increase in initial rate; a similar enhancement factor was observed for UiO-67-NH₂ vs. the parent UiO-67 compound (the difference between UiO-66 and UiO-67 is the use of biphenyldicarboxylate versus monophenyl-dicarboxylate as the linker).¹⁹ In addition to this work, we also compared the bidentate BDC linker with the tetradentate pyrene-based ligand of NU-1000 and observed a 2.3- and 23-fold increase in initial rate for the hydrated and dehydrated forms of NU-1000 vs.

UiO-66. We have attributed the larger of the rate enhancements to elimination of node-based aqua ligand substitution by the simulant as a rate-attenuating step, and secondarily to the presentation of a greater number of reactant accessible zirconium(IV) sites for NU-1000 versus UiO-66.²⁰

Table 1 summarizes the hydrolysis of methylparaoxon as a function of the MOF-based catalysts we have investigated to date.^{19,20,41} Given the remarkable efficacy of these MOFs towards this key chemical transformation, we were interested in further probing the mechanism of catalytic hydrolysis of methylparaoxon, in order to rationally design more active versions of these catalysts. Given their ease of synthesis, we herein return to the use of UiO-66 and UiO-67 to probe the catalysis mechanism (*vide infra*).

TABLE 1: Initial rates and half-lives of Zr-based MOFs used for hydrolysis of the nerve agent simulant methylparaoxon^{19,20,41}

MOF catalyst	Half-life (min)
UiO-66	35
UiO-66-NO ₂	45
UiO-66-(OH) ₂	60
UiO-66-NH ₂	1
UiO-67	4.5
UiO-67-NH ₂	2
UiO-67-NMe ₂	2
NU-1000	15
Dehydrated NU-1000	1.5

One common mechanism for the hydrolysis of methylparaoxon entails binding to a coordinatively unsaturated site on a Lewis-acidic metal cation, with concomitant weakening of phosphorous–oxygen bonds (or P–F in the case of Sarin); Figure 1c.^{23,42–50} A free or metal-bound hydroxide anion is then transferred to the phosphate. Subsequently, the now de-activated (i.e., non-toxic) product dissociates from the active site and the catalyst is regenerated. To probe the hy-

drolysis mechanism we varied the buffered solution OH^- concentration from 1.6×10^{-6} (pH = 8.3) to 2.0×10^{-4} (pH = 10.2), and followed the reaction kinetics. To our surprise, rather than accelerating with increasing $[\text{OH}^-]$, the rate of the catalytic reaction *decreased*. In contrast, the hydrolysis rate in the absence of a catalyst systematically increases with increasing hydroxide ion concentration. These observations point to differences in the mechanism for the catalyzed versus uncatalyzed reactions, beyond just Lewis acid weakening of substrate bonds.

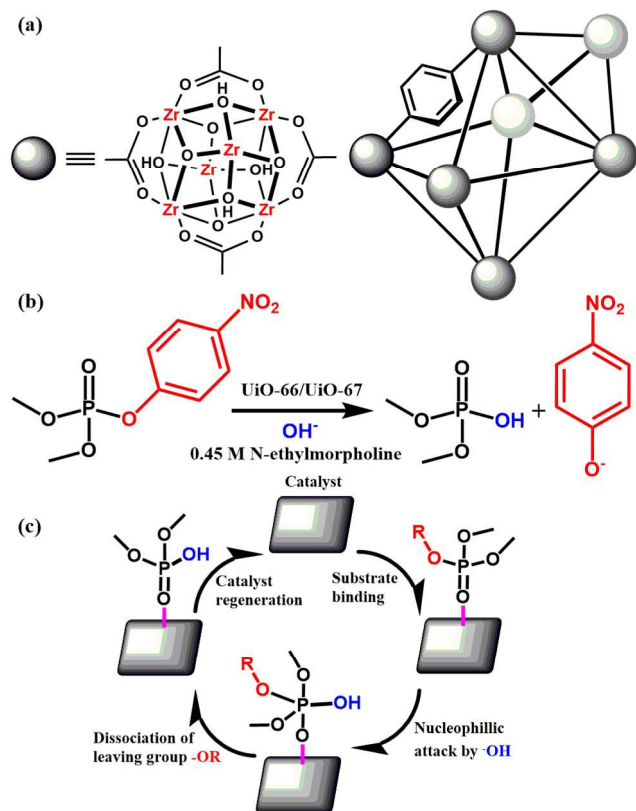


Figure 1: (a) Schematic of the node of UiO-66 (left) and the extended structure showing the relative positions of the octahedral and tetrahedral pores (right). (b) Reaction of methylparaoxon, a nerve-agent simulant with a MOF catalyst. (c) Generic mechanism for the catalytic hydrolysis of methylparaoxon.

Experimental

All reagents were purchased from commercial sources and used without further purification. UiO-66, dehydrated UiO-66 and UiO-67 were synthesized according to literature procedures.^{39,51}

Unless otherwise noted, hydrolysis experiments were carried out at room temperature as described previously.¹⁸ Briefly, to a solid sample of UiO-66 (2.5 mg, 6 mol %, 0.0015 mmole; 0.045 mole % of active surface sites) or UiO-67 (1 mg, 2 mol %, 0.0005 mmole) in an Eppendorf tube was added an aqueous solution of *N*-ethyl-morpholine (0.45 N) with additional acetic acid used to modulate the pH of the solution. The resulting mixture was stirred for 30 minutes to finely disperse the MOF particles. To the suspension was then added methylparaoxon (6.2 mg, 0.025 mmol). Periodic monitoring via UV-Vis spectroscopy was carried out by removing a 20 μL aliquot from the reaction mixture and diluting with an aqueous solution of *N*-ethyl-morpholine (10 mL, 0.45 M) prior to UV-

Vis measurements (Varian Cari 5000) (Figure 2). Progress of the reaction was monitored by following the *p*-nitrophenoxide absorbance at 407 nm to avoid overlapping absorptions with other species. No spectral evidence for the *p*-nitrophenol was observed at this pH (10.2). All background reactions were carried out under identical reaction conditions without the MOF catalyst.

Initial rates were determined using the method of initial rates.⁵² Polynomial fits of order 3–5 were used with the lowest observed correlation coefficient of 0.98.

Potentiometric titrations were completed with a Metrohm Titrando 905 equipped with Dosino 800 20 mL and 10 mL dosing units using procedures similar to those reported for $\text{Zr}(\text{OH})_4$.^{53,54} Prior to titration, approximately 50 mg of sample was mixed with approximately 60 mL of 0.01 M aq. NaNO_3 for 18 h. Each titration solution was adjusted using 0.1 M aq. HCl to a pH of 3, and was then titrated with 0.1 M aq. NaOH to a pH of 10.5. Titrations are run in triplicate.

Results and Discussions

Figure 2 illustrates the hydrolysis of methylparaoxon as a function of time and solution pH. Qualitatively, as the pH is lowered from 10.2 to 8.8, the overall reaction rate increases.⁵⁵ In contrast, the hydrolysis rate in the absence of a catalyst does not systematically increase with decreasing hydroxide ion concentration; see Figures S1 and S2 in the electronic supplementary information (ESI), suggesting a different mechanism for the MOF-catalyzed hydrolysis reaction versus the uncatalyzed hydrolysis reaction.

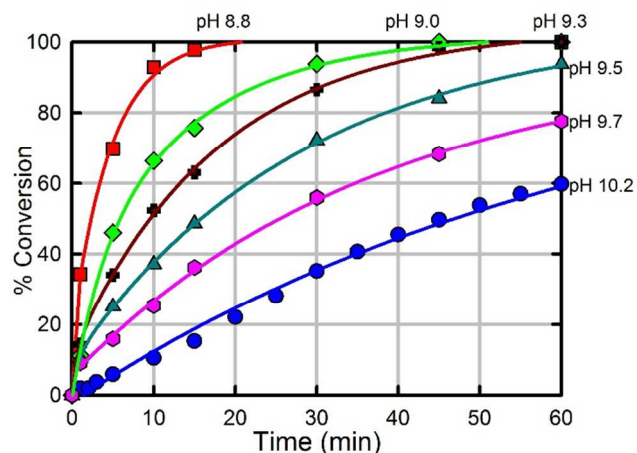


Figure 2: Hydrolysis rate of methylparaoxon, as measured via the formation of nitrophenoxide ($\lambda_{\text{max}} = 407 \text{ nm}$) as a function of time and pH for UiO-66; the buffer is 0.45 M *N*-ethyl-morpholine adjusted with acetic acid.

To quantitatively probe the $[\text{H}^+]$ dependence for the hydrolysis reaction, we applied the method of initial rates⁵² to each of the curves in Figure 2 (Figure 3). The rates, in units of formation of nitrophenoxide concentration per unit time are summarized in Table 2. Plotting the initial rates as a function of $[\text{H}^+]$ demonstrates, over the pH range of 8.8–9.7, that the hydrolysis reaction is first order in $[\text{H}^+]$ concentration or, equivalently, inverse-first-order in $[\text{OH}^-]$. At pH values below 8.8 the rate is independent of the $[\text{H}^+]$ concentration (Table 2). From the slope of the plot we obtain an observed rate constant of $4.6 \times 10^4 \text{ s}^{-1}$. These data suggest that the rate-limiting step, or a preceding step, involves proton transfer rather than hy-

droxide attack. These results are reminiscent of the results with UiO-66-NH₂ and UiO-67-NH₂, which show a similar enhancement due to the presence of a proximal Brønsted base. We suspect that the amino moiety may serve to modulate the pH proximal to the active site in a similar way to the experiments herein.⁵⁶

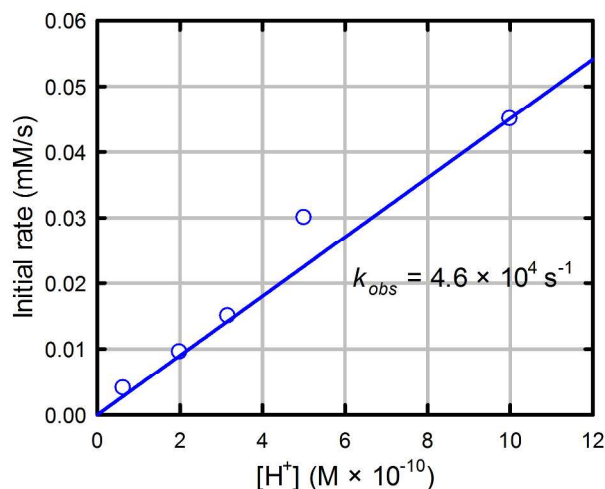


Figure 3: Plot of initial rate as a function of [H⁺] (or, equivalently, [OH⁻]⁻¹). The slope of the best-fit line gives an observed rate constant of $4.6 \times 10^4 \text{ s}^{-1}$.

Table 2: Initial rates and TOF for UiO-66 as a function of pH.

pH	Initial Rate (mM s ⁻¹)	TOF ^c _{all} (s ⁻¹)	TOF ^c _{surface} (s ⁻¹) ^a
10.2	0.0040	0.0026	0.35
9.7	0.0095	0.0063	0.84
9.5	0.015	0.0096	1.3
9.3	0.030	0.020	2.7
9.0	0.05 ^b	0.030	4.0
8.8	0.2 ^b	0.12	16
8.6	0.3 ^b	0.17	23
8.3	0.2 ^b	0.14	18

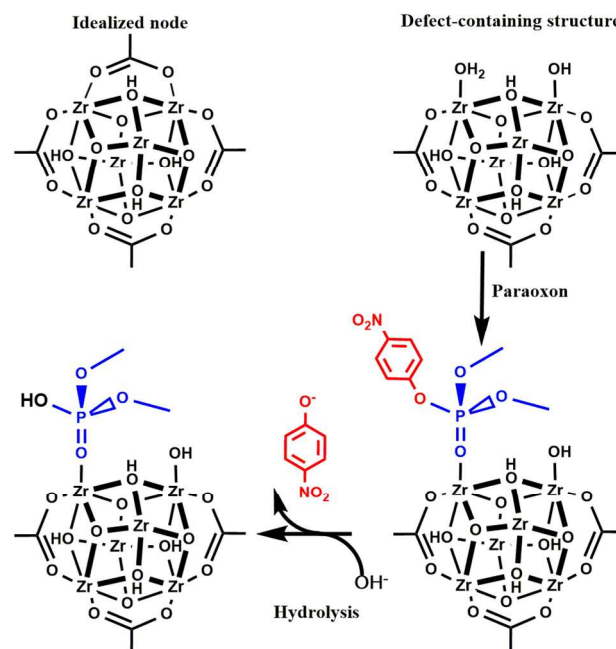
^aUiO-66 particles are 400 nm as synthesized. Due to the aperture size of UiO-66 and the relatively larger kinetic diameter of methylparaoxon, only the surface sites (ca. 0.75 % of the catalyst loading) are catalytically active.

^bA larger error is associated with these numbers due to the limited number of data points available for data fitting.

^cTurn-over frequency (TOF) is determined by dividing the initial rate (in mmole s⁻¹) by the catalyst loading (in mmoles) or external surface area adjusted catalyst loading (in mmoles).

To understand the pH dependence, we turned to the structure of UiO-66. Scheme 1 (top left) shows a UiO-66 node in idealized form. Given 12 linkers (some omitted for clarity), 4 μ₃-bridging hydroxides, and 4 μ₃-bridging oxo moieties, it is not possible for an organophosphate moiety to bind directly to a zirconium(IV)-center. For this small-aperture material, catalysis necessarily occurs on surface defects. It has been demonstrated elsewhere that conventionally synthesized UiO-66 contains only ~85% of the anticipated total amount of terephthalate linker.^{36,37,39,57} Further, each missing linker is

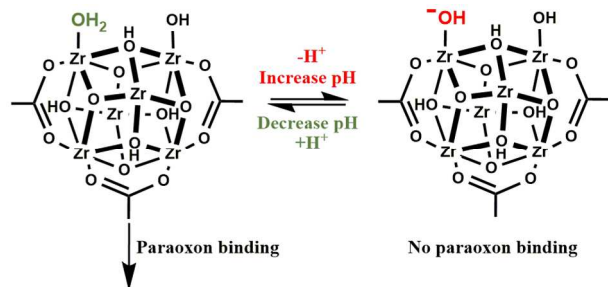
charge-compensated on the associated nodes by two coordinated hydroxides (one per node).^{36,37,39,57} The remaining coordination site on each node appears to be occupied by H₂O. The top right section of Scheme 1 shows a simplified representation (some linker carboxylates are again omitted for clarity). It is thus conceivable that surface defects, which are necessarily present even in the most pristine synthesis of UiO-66, take the same form as the internal defects. The proposed defect-site coordination is akin to that for MOFs containing eight-connected hexa-zirconium(IV) nodes.⁵⁸ We hypothesize that the coordinated neutral water molecule in Scheme 1 (top right) can be readily substituted by the neutral nerve agent (Scheme 1 bottom), but that the strongly ionically-bound hydroxide ligand cannot. Once aqua substitution has occurred, hydrolysis should rapidly follow. Calculations with NU-1000 and DMNP indicate that ligand substitution (DMNP for H₂O) followed by hydrolysis is downhill by 48 kJ mol⁻¹.²⁰



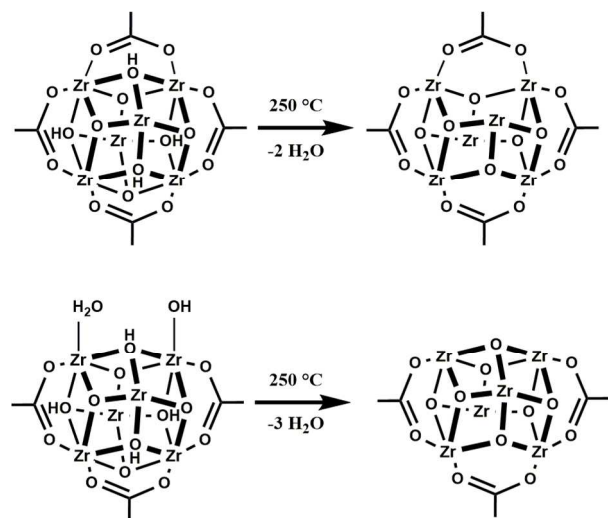
Scheme 1: (top left) Idealized node of UiO-66 showing no defects; eight out of 12 1,4-benzendicarboxylate (BDC) moieties removed for clarity. (top right) Presumed form of defect-containing cluster. (bottom) Proposed reaction mechanism between bound methylparaoxon and UiO-66 to form the hydrolyzed product, with substrate binding as the rate-limiting step. Omitted is fast release of the product from the node, a step that does *not* occur in the corresponding phosphotriesterase enzyme when the reactant is a fluorine-containing nerve agent.

One potential explanation for the pH-dependent reaction kinetics is illustrated in Scheme 2; at low H⁺ concentrations (i.e., high pH), ligated water molecules are largely converted to substitution-resistant hydroxo ligands. Thus, at solution pH values above the equivalence point value of the aqua ligand, only a minority of node sites will offer aqua ligands that are favorable towards ligand substitution. If methylparaoxon substitution for water is the rate-limiting step, then the overall hydrolysis reaction will become progressively faster with increasing [H⁺]. The results in Figures 1 and 2 are consistent with this picture, provided that the aqua titration endpoint value is between pH 9 or 10.

When the solution pH becomes low enough for the equilibrium in Scheme 2 to shift largely to the left, the hydrolysis reaction should become pH independent, and remain so for as long as methylparaoxon substitution remains the rate-determining step. The approximate invariance of reaction rates in Table 2 between pH 8.8 and 8.3 is consistent with this suggestion. Conversely, at very high pH, the fraction of available aqua ligands may become so low that the hydrolysis reaction proceeds via rate-limiting displacement of coordinated OH⁻ rather than H₂O, resulting in pH-independent kinetics. The rate entries in Table 2 for pH 9.7 and 10.2 suggest that at pH 10.2 the reaction is in or near this regime. Unfortunately, catalytic rate measurements at yet higher pH were not feasible.



Scheme 2: (left) Presumed composition of cluster in the absence of one BDC unit. Terminal hydroxide and aqua ligands fill the resulting open Zr(IV) coordination sites. At high pH values the aqua ligand converts to a substitution-resistant hydroxide, making the framework overall anionic.



Scheme 3: upon heating UiO-66 to 250 °C, a condensation reaction occurs between the hydroxides on the node. The new node structure of the perfect UiO-66 node is shown on the top,³⁹ and the proposed dehydrated defect-UiO-66 is shown on the right.

Given our hypothesis, we further examined the hydrolysis using dehydrated defect-UiO-66 as the catalyst. In dehydrated defect-UiO-66, terminal water and hydroxide ligands are removed. Following the behavior of NU-1000, the terminal hydroxide can be removed as a neutral water molecule by recruiting a proton from a bridging hydroxide; the cluster now has the formula Zr₆O₅(OH)₃⁺¹¹ and further contains two open sites on the zirconium node (Scheme 3). We anticipate that the dehydrated node will more readily bind the substrate. As can

be seen in Figure 4, catalysis with the dehydrated UiO-66 is roughly 10× faster than normal UiO-66; this finding is consistent with the mechanism in Scheme 2 and with our recent reported observations with NU-1000.²⁰

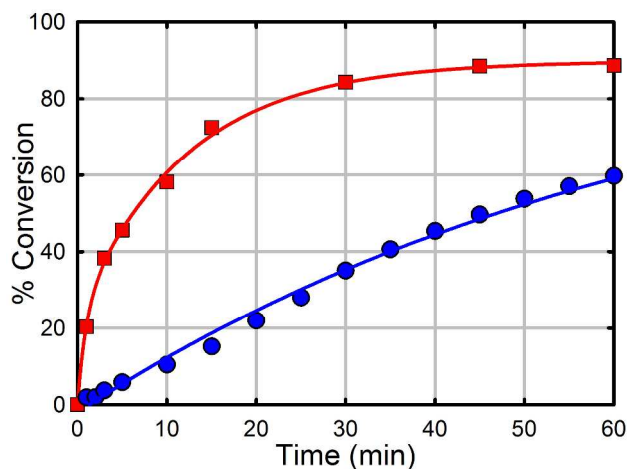


Figure 4: Hydrolysis rate of methylparaoxon using UiO-66 and dehydrated UiO-66 as the catalyst as measured via the formation of nitrophenoxide ($\lambda_{\text{max}} = 407 \text{ nm}$) as a function of time; the buffer is 0.45 M *N*-ethyl-morpholine.

In order to further probe the proposed mechanism shown in scheme 2, we turned our attention to potentiometric titration of UiO-66. Figure 5 presents the change in pH of a solution containing UiO-66 as a function of NaOH addition. Notably, the curve reveals an equivalence point at 9.34, i.e., about the value expected for the proposed reaction scheme.⁵⁹

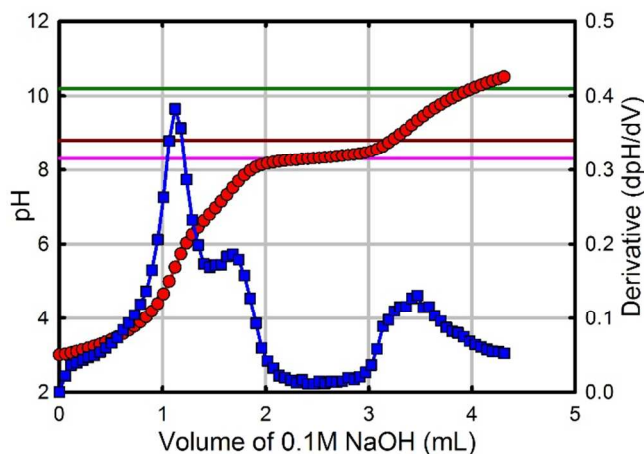


Figure 5: Potentiometric titration of UiO-66. The dark-green and dark-red cross lines the pH values of 10.2 and 8.8, respectively, which corresponds to the pH range in which there is a linear correlation between [H⁺] and initial rate. The pink line (pH 8.3) indicates the lowest pH examined for the hydrolysis of UiO-66.

Finally, we extended the hydrolysis rate studies to reactions catalyzed by UiO-67 (Figures S3–S7 and Table S1 in the ESI), a close structural analogue of UiO-66. We have recently observed that UiO-67 elicits significantly faster methylparaoxon hydrolysis than does UiO-66. With identical catalyst loading, UiO-67 engenders a 6-fold faster initial rate ($t_{1/2} = 4.5 \text{ min}$) than does UiO-66. When used at half the catalyst loading of UiO-66, it induces a ca. 2-fold faster initial rate ($t_{1/2} = 15 \text{ min}$).

Given the faster hydrolysis, we examined the pH dependence of the reaction rate at 0.5 μmole catalyst loading (vs. 1.5 μmole for UiO-66). As shown in Figures S3–S4 and Table S1 (see ESI), and like the behavior with UiO-66, the UiO-67-catalyzed hydrolysis rate increases with decreasing pH, yielding an apparent rate constant essentially identical to that for UiO-66 (but at one-third the loading of UiO-66).⁵⁵ Furthermore, although it is has been reported that UiO-67 is unstable in water, in our hands, UiO-67 showed no such instability.⁶⁰ Figures S5–S6 in the ESI shows the powder X-ray diffractograms and nitrogen sorption isotherms of UiO-67 pre- and post-catalysis. The diffractograms look identical to one another and the decrease in surface area (2300 m^2/g to 1020 m^2/g) is attributed to pore clogging from the hydrolysis products; similar decreases in surface area have been observed for phosphate modified Zr_6 -based nodes.^{61,62} Furthermore, filtration of the MOF mid-catalysis ceased the catalytic reaction. In addition, inductively coupled plasma mass spectrometry of the supernate showed no evidence of leached zirconium. Thus, the active catalyst is UiO-67.

Conclusions

The hydroxide driven hydrolysis of the nerve-agent simulant, methylparaoxon, has recently been shown to be catalyzed by UiO-66 and -67 in buffered solutions at pH = 10. In contrast to the uncatalyzed reaction, and to what might otherwise be expected for a hydroxide-consuming reaction, the catalyzed reaction accelerates as the OH^- concentration is lowered or, equivalently, the hydronium concentration is increased. The unexpected behavior can be understood in terms of rate-limiting simulant displacement of a zirconium-ligated water molecule at a defect site (i.e., missing-linker site) on the MOF node. Once bound to a highly Lewis acidic zirconium(IV) node site, the phosphorous–oxygen bonds of the substrate weaken, with the weakest of the bonds succumbing to nucleophilic attack by hydroxide in a step that is fast compared with the aqua-displacement/substrate-binding step.

At sufficiently high pH, the majority of the MOF aqua ligands are converted to substitution-resistant hydroxo ligands. Lowering the solution pH progressively returns them to aqua form and, therefore, increases the rate of methylparaoxon substitution and the overall rate of hydrolysis. When the pH is low enough (ca. pH 8.8) for nearly all the OH^- ligands to be converted to ligated water, the rate of the methylparaoxon binding step, and therefore, the overall reaction, become pH independent. Support for this scheme is provided by potentiometric titrations showing endpoint values of 9.3 and 9.7, respectively, for UiO-66 and -67. If further investigations indicate that the corresponding pK_a values track with these endpoint values, then it is tempting to ascribe the observed 3- to 6-fold rate difference to this pK_a difference. Control over binding-site protonation, perhaps via local buffering with pendant bases, may provide a means for further accelerating MOF-catalyzed reactions. We are currently exploring this and related ideas.

AUTHOR INFORMATION

Corresponding Author

*j-hupp@u.northwestern.edu; o-farha@northwestern.edu;

Author Contributions

The manuscript was written through contributions of all authors. / All authors have given approval to the final version of the manuscript.

Funding Sources

O.K.F. and J.T.H. gratefully acknowledge DTRA for financial support (grant HDTRA-1-10-0023).

SUPPORTING INFORMATION

Supporting Information Available: Uncatalyzed reaction rate and pH dependence, hydrolysis rate and pH dependence using UiO-67, powder x-ray diffractograms and surface area analysis of UiO-67 pre/post catalysis, and potentiometric titration of UiO-67. This material is available free of charge via the Internet at <http://pubs.acs.org>.

REFERENCES

- (1) Yaghi, O. M.; O'Keefe, M.; Ockwig, N. W.; Chae, H. K.; Eddaoudi, M.; Kim, J. *Nature* **2003**, *423*, 705.
- (2) Férey, G. *Chemical Society Reviews* **2008**, *37*, 191.
- (3) Horike, S.; Shimomura, S.; Kitagawa, S. *Nat. Chem.* **2009**, *1*, 695.
- (4) Farrusseng, D. *Metal-Organic Frameworks: Applications from Catalysis to Gas Storage*; Wiley-VCH, 2011.
- (5) He, Y.; Song, C.; Ling, Y.; Wu, C.; Krishna, R.; Chen, B. *APL Mater.* **2014**, *2*, 124102.
- (6) Stephenson, C. J.; Beyzavi, M. H.; Klet, R. C.; Hupp, J. T.; Farha, O. K. *APL Mater.* **2014**, *2*, 123901.
- (7) Kreno, L. E.; Leong, K.; Farha, O. K.; Allendorf, M.; Van Duyne, R. P.; Hupp, J. T. *Chemical Reviews* **2012**, *112*, 1105.
- (8) Zhou, H.-C. J.; Kitagawa, S. *Chemical Society Reviews* **2014**, *43*, 5415.
- (9) DeCoste, J. B.; Weston, M. H.; Fuller, P. E.; Tovar, T. M.; Peterson, G. W.; LeVan, M. D.; Farha, O. K. *Angewandte Chemie International Edition* **2014**, *53*, 14092.
- (10) DeCoste, J. B.; Peterson, G. W. *Chemical reviews* **2014**, *114*, 5695.
- (11) Eddaoudi, M.; Sava, D. F.; Eubank, J. F.; Adil, K.; Guillerme, V. *Chemical Society reviews* **2014**, *44*, 228.
- (12) Rodenas, T.; Luz, I.; Prieto, G.; Seoane, B.; Miro, H.; Corma, A.; Kapteijn, F.; Llabrés, F. X.; Gascon, J. *Nat. Mater.* **2015**, *14*, 48.
- (13) So, M. C.; Wiederrecht, G. P.; Mondloch, J. E.; Hupp, J. T.; Farha, O. K. *Chemical Communications* **2015**, *51*, 3501.
- (14) Li, J.-R.; Sculley, J.; Zhou, H.-C. *Chemical reviews* **2012**, *112*, 869.
- (15) Farha, O. K.; Yazaydin, A. Ö.; Eryazici, I.; Malliakas, C. D.; Hauser, B. G.; Kanatzidis, M. G.; Nguyen, S. T.; Snurr, R. Q.; Hupp, J. T. *Nat. Chem.* **2010**, *2*, 944.
- (16) Wilmer, C. E.; Farha, O. K.; Yildirim, T.; Eryazici, I.; Krungleviciute, V.; Sarjeant, A. A.; Snurr, R. Q.; Hupp, J. T. *Energy & Environmental Science* **2013**, *6*, 1158.
- (17) Lu, G.; Farha, O. K.; Zhang, W.; Huo, F.; Hupp, J. T. *Advanced Materials* **2012**, *24*, 3970.
- (18) Katz, M. J.; Mondloch, J. E.; Totten, R. K.; Park, J. K.; Nguyen, S. T.; Farha, O. K.; Hupp, J. T. *Angewandte Chemie International Edition* **2014**, *53*, 497.
- (19) Katz, M. J.; Moon, S.-Y.; Mondloch, J. E.; Beyzavi, M. H.; Stephenson, C. J.; Hupp, J. T.; Farha, O. K. *Chemical Science* **2015**, *6*, 2286.
- (20) Mondloch, J. E.; Katz, M. J.; Isley III, W. C.; Ghosh, P.; Liao, P.; Bury, W.; Wagner, G. W.; Hall, M. G.; DeCoste, J. B.; Peterson, G. W.; Snurr, R. Q.; Cramer, C. J.; Hupp, J. T.; Farha, O. K. *Nat. Mater.* **2015**, *14*, 512.
- (21) Zou, R.; Zhong, R.; Han, S.; Xu, H.; Burrell, A. K.; Henson, N.; Cape, J. L.; Hickmott, D. D.; Timofeeva, T. V.; Larson, T. E.; Zhao, Y. *Journal of the American Chemical Society* **2010**, *132*, 17996.
- (22) Nunes, P.; Gomes, A. C.; Pillinger, M.; Gonçalves, I. S.; Abrantes, M. *Microporous and Mesoporous Materials* **2015**, *208*, 21.
- (23) Zhu, X.; Li, B.; Yang, J.; Li, Y.; Zhao, W.; Shi, J.; Gu, J. *ACS applied materials & interfaces* **2015**, *7*, 223.
- (24) Pita, R.; Domingo, J. *Toxics* **2014**, *2*, 391.

- (25) Wang, S.; Bromberg, L.; Schreuder-Gibson, H.; Hatton, T. A. *ACS applied materials & interfaces* **2013**, *5*, 1269.
- (26) Totten, R. K.; Weston, M. H.; Park, J. K.; Farha, O. K.; Hupp, J. T.; Nguyen, S. T. *ACS Catal.* **2013**, *3*, 1454.
- (27) Totten, R. K.; Kim, Y.-S.; Weston, M. H.; Farha, O. K.; Hupp, J. T.; Nguyen, S. T. *Journal of the American Chemical Society* **2013**, *135*, 11720.
- (28) Kamerlin, S. C. L.; Sharma, P. K.; Prasad, R. B.; Warshel, A. *Quarterly reviews of biophysics* **2013**, *46*, 1.
- (29) Enserink, M. *Science* **2013**, *341*, 1050.
- (30) Totten, R. K.; Ryan, P.; Kang, B.; Lee, S. J.; Broadbelt, L. J.; Snurr, R. Q.; Hupp, J. T.; Nguyen, S. T. *Chemical communications* **2012**, *48*, 4178.
- (31) Yang, Y.-C. *Accounts of Chemical Research* **1999**, *32*, 109.
- (32) Anzueto, A.; deLemos, R. A.; Seidenfeld, J.; Moore, G.; Hamil, H.; Johnson, D.; Jenkinson, S. G. *Fundamental and Applied Toxicology* **1990**, *14*, 676.
- (33) Millard, C. B.; Kryger, G.; Ordentlich, A.; Greenblatt, H. M.; Harel, M.; Raves, M. L.; Segall, Y.; Barak, D.; Shafferman, A.; Silman, I.; Sussman, J. L. *Biochemistry* **1999**, *38*, 7032.
- (34) Katz, M. J.; Brown, Z. J.; Colón, Y. J.; Siu, P. W.; Scheidt, K. A.; Snurr, R. Q.; Hupp, J. T.; Farha, O. K. *Chemical Communications* **2013**, *49*, 9449.
- (35) Cavka, J. H.; Jakobsen, S.; Olsbye, U.; Guillou, N.; Lamberti, C.; Bordiga, S.; Lillerud, K. P. *Journal of the American Chemical Society* **2008**, *130*, 13850.
- (36) Shearer, G. C.; Chavan, S.; Ethiraj, J.; Vitillo, J. G.; Svelle, S.; Olsbye, U.; Lamberti, C.; Bordiga, S.; Lillerud, K. P. *Chemistry of Materials* **2014**, *26*, 4068.
- (37) Øien, S.; Wragg, D.; Reinsch, H.; Svelle, S.; Bordiga, S.; Lamberti, C.; Lillerud, K. P. *Crystal Growth and Design* **2014**, *14*, 5370.
- (38) Chavan, S.; Vitillo, J. G.; Gianolio, D.; Zavorotynska, O.; Civalleri, B.; Jakobsen, S.; Nilsen, M. H.; Valenzano, L.; Lamberti, C.; Lillerud, K. P.; Bordiga, S. *Physical chemistry chemical physics* **2012**, *14*, 1614.
- (39) Valenzano, L.; Civalleri, B.; Chavan, S.; Bordiga, S.; Nilsen, M. H.; Jakobsen, S.; Lillerud, K. P.; Lamberti, C. *Chemistry of Materials* **2011**, *23*, 1700.
- (40) Kandiah, M.; Nilsen, M. H.; Usseglio, S.; Jakobsen, S.; Olsbye, U.; Tilset, M.; Larabi, C.; Quadrelli, E. A.; Bonino, F.; Lillerud, K. P. *Chemistry of Materials* **2010**, *22*, 6632.
- (41) Katz, M. J.; Mondloch, J. E.; Totten, R. K.; Park, J. K.; Nguyen, S. T.; Farha, O. K.; Hupp, J. T. *Angewandte Chemie International Edition* **2013**, *53*, 497.
- (42) Duarte, F.; Aqvist, J.; Williams, N. H.; Kamerlin, S. C. L. *Journal of the American Chemical Society* **2015**, *137*, 1081.
- (43) Kirby, A. J.; Jencks, W. P. *Journal of the American Chemical Society* **1965**, *87*, 3209.
- (44) Lewis, V. E.; Donarski, W. J.; Wild, J. R.; Raushel, F. M. *Biochemistry* **1988**, *27*, 1591.
- (45) Kimura, E. *Current Opinion in Chemical Biology* **2000**, *4*, 207.
- (46) Aubert, S. D.; Li, Y.; Raushel, F. M. *Biochemistry* **2004**, *43*, 5707.
- (47) Imhof, P.; Fischer, S.; Krämer, R.; Smith, J. C. *Journal of Molecular Structure: THEOCHEM* **2005**, *713*, 1.
- (48) Aguilar-Pérez, F.; Gómez-Tagle, P.; Collado-Fregoso, E.; Yatsimirsky, A. K. *Inorganic chemistry* **2006**, *45*, 9502.
- (49) Liu, T.; Neverov, A. A.; Tsang, J. S. W.; Brown, R. S. *Organic & Biomolecular Chemistry* **2005**, *3*, 1525.
- (50) Klinkel, K. L.; Kiemele, L. A.; Gin, D. L.; Hagadorn, J. R. *Chemical Communications* **2006**, *1*, 2919.
- (51) Katz, M. J.; Brown, Z. J.; Colón, Y. J.; Siu, P. W.; Scheidt, K. A.; Snurr, R. Q.; Hupp, J. T.; Farha, O. K. *Chem. Commun.* **2013**, *49*, 9449.
- (52) Casado, J.; Lopez-Quintela, M. A.; Lorenzo-Barral, F. M. *Journal of Chemical Education* **1986**, *63*, 450.
- (53) Glover, T. G.; Peterson, G. W.; Decoste, J. B.; Browe, M. A. *Langmuir* **2012**, *28*, 10478.
- (54) Bandoz, T. J.; Laskoski, M.; Mahle, J.; Mogilevsky, G.; Peterson, G. W.; Rossin, J. A.; Wagner, G. W. *Journal of Physical Chemistry C* **2012**, *116*, 11606.
- (55) Under our experimental conditions, the hydrolysis of methylparaoxon by Zr(OH)₄ is negligible
- (56) Due to the rapid hydrolysis observed with UiO-66-NH₂ as well as the presence of a proximal base on the catalyst, attempts to determine if a pH dependence exists for UiO-66-NH₂ were inconclusive.
- (57) Cliffe, M. J.; Wan, W.; Zou, X.; Chater, P. a.; Kleppe, A. K.; Tucker, M. G.; Wilhelm, H.; Funnell, N. P.; Coudert, F.-X.; Goodwin, A. L. *Nature communications* **2014**, *5*, 4176.
- (58) Planas, N.; Mondloch, J. E.; Tussupbayev, S.; Borycz, J.; Cramer, C. J.; Hupp, J. T.; Farha, O. K.; Gagliardi, L. *J. Phys. Chem. Lett.* **2014**, *5*, 3716.
- (59) Additionally observed equivalence points are present at pH 5.38 and 7.51; their assignment must await additional work.
- (60) Mondloch, J. E.; Katz, M. J.; Planas, N.; Semrouni, D.; Gagliardi, L.; Hupp, J. T.; Farha, O. K. *Chemical communications* **2014**, *50*, 8944.
- (61) Deria, P.; Bury, W.; Hod, I.; Kung, C.-W.; Karagiari, O.; Hupp, J. T.; Farha, O. K. *Inorganic Chemistry* **2015**, *54*, 2185.
- (62) We have collected NMR data to show that there are 2-4 units of nitrophenol as well as dimethylphosphate in post-catalysis MOF NMRs. We attribute the decrease in surface area of UiO-67 to the presence of these moieties in the pore.

Table of Contents artwork

